Eur. Phys. J. D (2014) 68: 171
DOI: 10.1140/epjd/e2014-40765-7

THE EUROPEAN PHYSICAL JOURNAL D

Regular Article

Analytical solutions for diatomic Rydberg quasimolecules in a laser field

Nikolay Kryukov and Eugene Oks[a]

Physics Department, 206 Allison Lab., Auburn University, Auburn, AL 36849, USA

Received 6 December 2013 / Received in final form 9 April 2014
Published online 27 June 2014 –

Abstract. In our previous works we studied analytically helical Rydberg states and circular Rydberg states of two-Coulomb-center systems consisting of two nuclei of charges Z and Z', separated by a distance R, and one electron. We obtained energy terms of these Rydberg quasimolecules for a field-free case, as well as under a static electric field or under a static magnetic field. In the present paper we study such systems under a laser field. For the situation where the laser field is linearly-polarized along the internuclear axis, we found an analytical solution for the stable helical motion of the electron valid for wide ranges of the laser field strength and frequency. We also found resonances, corresponding to a laser-induced unstable motion of the electron, that result in the destruction of the helical states. For the situation where such Rydberg quasimolecules are under a circularly-polarized field, polarization plane being perpendicular to the internuclear axis, we found an analytical solution for circular Rydberg states valid for wide ranges of the laser field strength and frequency. We showed that both under the linearly-polarized laser field and under the circularly-polarized laser field, in the electron radiation spectrum in the addition to the primary spectral component at (or near) the unperturbed revolution frequency of the electron, there appear satellites. We found that for the case of the linearly-polarized laser field, the intensities of the satellites are proportional to the squares of the Bessel functions $J_q^2(s)$, $(q = 1, 2, 3, \ldots)$, where s is proportional to the laser field strength. As for the case of the circularly-polarized field, we demonstrated that there is a red shift of the primary spectral component – the shift linearly proportional to the laser field strength. Under a laser field of a known strength, in the case of the linear polarization the observation of the satellites would be the confirmation of the helical electronic motion in the Rydberg quasimolecule, while in the case of the circular polarization the observation of the red shift of the primary spectral component would be the confirmation of the specific type of the phase modulation of the electronic motion. Conversely, if the laser field strength is unknown, both the relative intensities of the satellites and the red shift of the primary spectral component could be used for measuring the laser field strength.

1 Introduction

Circular states of atomic and molecular systems in general, as well as circular Rydberg states (CRS) in particular, have been extensively studied both theoretically and experimentally for several reasons (see, e.g., [1–17] and references therein). Namely: (a) they have long radiative lifetimes and highly anisotropic collision cross sections, thereby enabling experiments on inhibited spontaneous emission and cold Rydberg gases, (b) these classical states correspond to quantal coherent states, objects of fundamental importance, (c) a classical description of these states is the primary term in the quantal method based on the $1/n$-expansion.

In our previous works [2,4,7,11,12,14,15] we studied analytically circular Rydberg states of two-Coulomb-center systems consisting of two nuclei of charges Z and Z', separated by a distance R, and one electron. We obtained energy terms of these Rydberg quasimolecules for a field-free case [14,15], as well as under a static electric field [2] or under a static magnetic field [11], and studied crossings of the energy terms – the crossings that enhance charge exchange in these systems.

Our analysis was not confined to circular orbits of the electron. For example, in paper [15] we studied in detail *helical* Rydberg states of these Rydberg quasimolecules. In order to make those results more transparent, we briefly outline here the scheme of that analysis. In cylindrical coordinates (z, ρ, φ) with the z-axis along the internuclear axis, using the axial symmetry of the problem, the z- and ρ-motions can be separated from the φ-motion. The φ-motion can be then determined from the calculated ρ-motion. Equilibrium points of the two-dimensional motion in the $z\rho$-space were studied and a condition distinguishing between two physically different cases, where the effective potential energy either has a two-dimensional

[a] e-mail: goks@physics.auburn.edu

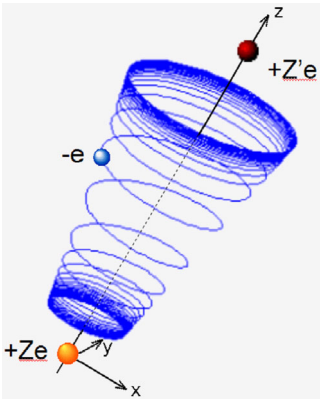

Fig. 1. Sketch of the helical motion of the electron in the ZeZ'-system at the absence of the magnetic field. We stretched the trajectory along the internuclear axis to make its details better visible.

minimum in the $z\rho$-space or has a saddle point in the $z\rho$-space, was explicitly derived. In particular, it turned out that the boundary between these two cases corresponds to the point of crossing of the upper and middle energy terms (out of the three energy terms in this system). For the stable motion, the trajectory was found to be a helix on the surface of a cone, with axis coinciding with the internuclear axis. In this *helical* state, the electron, while spiraling on the surface of the cone, oscillates between two end-circles which result from cutting the cone by two parallel planes perpendicular to its axis (Fig. 1).

In the present paper we study such Rydberg quasimolecules under a laser field. For the situation where the laser field is linearly-polarized along the internuclear axis, we found an analytical solution for the stable helical motion of the electron valid for wide ranges of the laser field strength and frequency. We also found resonances, corresponding to a laser-induced unstable motion of the electron, that result in the destruction of the helical states. For the situation where such Rydberg quasimolecules are under a circularly-polarized field, polarization plane being perpendicular to the internuclear axis, we found an analytical solution for circular Rydberg states valid for wide ranges of the laser field strength and frequency. We showed that both under the linearly-polarized laser field and under the circularly-polarized laser field, in the electron radiation spectrum in the addition to the primary spectral component at (or near) the unperturbed revolution frequency of the electron, there appear satellites. We found that for the case of the linearly-polarized laser field, the intensities of the satellites are proportional to the squares of the Bessel functions $J_q^2(s)$, $(q = 1, 2, 3, \ldots)$, where s is proportional to the laser field strength. As for the case of the circularly-polarized field, we demonstrated that there is a red shift of the primary spectral component – the shift linearly proportional to the laser field strength.

We note that quasimolecules based on two ions of different nuclear charges occur in various plasma experiments. Examples are (but not limited to) the following. First, in magnetically-controlled fusion machines (such as, e.g., tokamaks) in addition to the very low-Z ions originating from the fuel and/or from injected neutral beams, there occur naturally impurity ions of significantly higher nuclear charges. Second, in laser-controlled fusion experiments heavy dopants are frequently added to the deuterium/tritium fuel for plasma diagnostics, resulting in the similar situation. Third, plasmas containing ions of different nuclear charges are created in those studies of laser-plasma interaction where the laser radiation is incident on solid targets composed of several chemical elements. The fourth example relates to the interaction of the solar wind, consisting of multicharged ions, with low-Z matter within the heliosphere.

Since Rydberg atoms form commonly in plasmas due to the recombination of electrons and positive ions, then the formation of Rydberg quasimolecules, considered in the present paper, becomes possible in plasmas containing ions of different nuclear charges. Specifically, in tokamak plasmas, the interaction of a neutral beam of hydrogen or helium (injected for heating and/or diagnostics) with naturally occurring fully-stripped impurity ions of significantly higher nuclear charges result in charge exchange. Due to the resonant nature of the process, electrons are predominantly transferred to Rydberg states of the impurity ions (see, e.g. [18]), thus facilitating the existence of one-electron Rydberg quasimolecules. Since these are highly-excited states ($n \gg 1$), it is appropriate using the classical description of these states as the primary term in the quantal method based on the $1/n$-expansion.

2 Analytical solution for the case of a linearly-polarized laser field

We consider the case where the laser is polarized parallel to the internuclear axis and oscillates sinusoidally with the frequency ω. The projection L of the angular momentum on the internuclear axis is conserved here due to φ-symmetry. The corresponding Hamiltonian is:

$$H = \frac{p_\rho^2 + p_z^2}{2} + \frac{L^2}{2\rho^2} - \frac{Z}{\sqrt{\rho^2 + z^2}} - \frac{Z'}{\sqrt{\rho^2 + (R - z)^2}} + zF\cos\omega t. \quad (1)$$

Below we scale all frequencies using the factor $(R^3/Z)^{1/2}$: for example, the scaled laser frequency is $\mu = \omega(R^3/Z)^{1/2}$. We also use scaled coordinates as in our papers [14,15]

$$w = \frac{z}{R}, \quad v = \frac{\rho}{R} \quad (2)$$

where R is the internuclear distance. The origin is at the location of charge Z.

Without the electric field, in an equilibrium orbit, the motion occurs on the φ-coordinate, while the z- and ρ-coordinates do not change (their time derivatives vanish). Thus, for this orbit the first term vanishes in (1), as well as the last one (due to no electric field), and the

remaining terms constitute the electron's equilibrium energy. Taking the derivatives with respect to the z- and ρ-coordinates and setting them equal to zero, we obtain the equilibrium values of the angular momentum and the ρ-coordinate at any allowed value of the z-coordinate for a given ratio of charges $b = Z'/Z$.

In the vicinity of the equilibrium the motion in $z\rho$-space corresponds to a two-dimensional harmonic oscillator [15]. Its scaled eigen-frequencies are

$$\omega_{\pm} = \frac{1}{\left(w^2 + v_0^2\right)^{3/4}} \sqrt{\frac{1}{1-w} \pm \frac{3w}{\sqrt{\left(w^2 + v_0^2\right)\left(\left(1-w\right)^2 + v_0^2\right)}}} \tag{3}$$

where the equilibrium value of v (denoted as v_0) is connected to w as follows [14,15]:

$$v_0(w,b) = \sqrt{\frac{w^{2/3}(1-w)^{4/3} - b^{2/3}w^2}{b^{2/3} - w^{2/3}(1-w)^{-2/3}}} \tag{4}$$

(we remind that $b = Z'/Z$). The motion occurs on the axes (w', v'), which are the original axes (w, v) rotated by an angle α given in [15]. The dependence of the angle α on the scaled coordinate w can be expressed in the most compact form by introducing the notation:

$$\gamma = \left(\frac{1}{w} - 1\right)^{1/3}. \tag{5}$$

In the γ-representation it has the form

$$\alpha = \frac{1}{2}\,\mathrm{arctg}\,\frac{\sqrt{\left(b^{2/3}\gamma^2 - 1\right)\left(\gamma^4 - b^{2/3}\right)}}{\gamma\left(b^{2/3} + \gamma\right)}. \tag{6}$$

The scaled eigen-frequencies ω_- and ω_+ are the scaled frequencies of small oscillations about the equilibrium along the coordinates w', v' accordingly.

As we introduce the oscillating electric field, these oscillations become forced, with the forces $F\cos\alpha\cos\omega t$ on w' and $F\sin\alpha\cos\omega t$ on v'. Therefore, the deviations from equilibrium on (w', v') are (see, e.g., textbooks [19,20])

$$\delta w' = \frac{f\cos\alpha}{\omega_-^2 - \mu^2}\cos\mu\tau, \delta v' = \frac{f\sin\alpha}{\omega_+^2 - \mu^2}\cos\mu\tau \tag{7}$$

where $f = F(R^2/Z)$, $\mu = \omega(R^3/Z)^{1/2}$ and $\tau = t(Z/R^3)^{1/2}$. Now we revert to the original coordinates (w, v) and obtain the equations of motion in the linearly-polarized oscillatory electric field in the vicinity of the equilibrium: the electron follows the circular path corresponding to the case with no electric field with deviations from equilibrium depending on the scaled time τ:

$$\begin{aligned}\delta w &= f\left(\frac{\cos^2\alpha}{\omega_-^2 - \mu^2} + \frac{\sin^2\alpha}{\omega_+^2 - \mu^2}\right)\cos\mu\tau,\\ \delta v &= f\sin\alpha\cos\alpha\left(\frac{1}{\omega_-^2 - \mu^2} - \frac{1}{\omega_+^2 - \mu^2}\right)\cos\mu\tau\end{aligned} \tag{8}$$

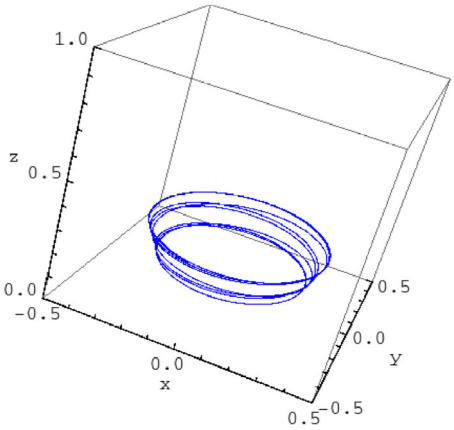

Fig. 2. The calculated trajectory of the electron in the linearly-polarized laser field for $b = 3$, $f = 1$, $\mu = 1$ at $w = 0.2$. The z-axis is along the internuclear axis.

From equation (8) it is seen that the strength and frequency of the laser field affect the amplitudes of the forced oscillations on w- and v-axes; in fact, these amplitudes are proportional to the field strength f. The frequencies of the forced oscillations on the axes are equal to that of the laser field, instead of ω_- and ω_+.

Since the Hamiltonian from equation (1) does not depend on φ, the corresponding momentum is conserved:

$$p_\varphi = \rho^2\frac{d\varphi}{dt} \equiv L = \mathrm{const}. \tag{9}$$

We can re-write equation (9) in the scaled notations as:

$$\frac{d\varphi}{d\tau} = \frac{l}{v^2(\tau)} \tag{10}$$

where $\ell = L/(ZR)^{1/2}$ is the scaled angular momentum. Substituting in equation (10) $v(\tau) = v + \delta v(\tau)$, where $v(w)$ is the equilibrium value of the scaled radius v of the electron orbit from equation (4) and $\delta v(\tau)$ is given by equation (8), we obtain

$$\frac{d\varphi}{dt} \approx \frac{l}{v_0^2} - \frac{2l}{v_0^3}\delta v(\tau) \tag{11}$$

which after the integration with respect to time yields:

$$\varphi(t) \approx \frac{l}{v_0^2}\tau - \frac{2l}{\mu v_0^3} f\sin\alpha\cos\alpha\left(\frac{1}{\omega_-^2 - \mu^2} - \frac{1}{\omega_+^2 - \mu^2}\right)\sin\mu\tau. \tag{12}$$

From equation (12) it is seen that the φ-motion is a rotation about the internuclear axis with the scaled frequency ℓ/v^2, slightly modulated by oscillations of the scaled radius of the orbit v at the laser frequency μ (i.e., at the laser frequency ω in the usual notation).

Thus, from equations (8) and (12) it is clear that the electron is bound to a conical surface which incorporates the original circular orbit. In Figure 2 below the calculated three-dimensional trajectory is plotted for $b = 3$, $f = 1$, $\mu = 1$ at $w = 0.2$.

The expression for $\varphi(\tau)$ from equation (12), i.e., $\varphi[t(Z/R^3)^{1/2}]$, enters the following Fourier-transform that determines the amplitude of the power spectrum of the electron radiation

$$A_l(\Delta) = \frac{1}{\pi}\int_0^\infty dt\,\cos\left(\Delta t - \varphi\left(t\sqrt{\frac{Z}{R^3}}\right)\right) \qquad (13)$$

where Δ is the radiation frequency measured, e.g., by a spectrometer. This is the standard expression for the case of a phase modulation of the atomic oscillator (see, e.g., [21]). The sinusoidal modulation of the phase φ is analogous to the situation where hydrogen spectral lines are modified by an external monochromatic field at the frequency ω, the latter problem being solved analytically by Blochinzew as early as in 1933 [22] (a further study can be found, e.g., in book [23]).

From Blochinzew's results it follows for our case in the electron radiation spectrum, this helical motion should manifest as follows. The most intense emission would be at the frequency $\Omega = d\varphi/dt$ of the rapid φ-motion. In addition, there will be satellites at the frequencies $\Omega \pm q\omega$, where $q = 1, 2, 3, \ldots$, whose relative intensities I_q are controlled by the Bessel functions $J_q(s)$:

$$I_q = (J_q(s))^2,\ s = \frac{2l}{\mu v_0^3} f \sin\alpha\cos\alpha\left(\frac{1}{\omega_-^2-\mu^2} - \frac{1}{\omega_+^2-\mu^2}\right). \qquad (14)$$

The oscillatory motion of the electron in the $z\rho$-space with the laser frequency ω should lead also to the radiation at this frequency. However, since $\omega \ll \Omega$, this spectral component would be far away from the primary spectral line and its satellites.

From equation (8) it is also seen that there are resonances when the laser frequency is equal to one of the eigen-frequencies of the motion in the $z\rho$-space, i.e., when either $\mu = \omega_+$ or $\mu = \omega_-$. It turns out that these conditions yield three resonance points on the w-axis for the laser field frequency μ below a certain critical value μ_c, or five resonance points for $\mu > \mu_c$ – see the figures below. (We note that the regions, where $\omega_+(w)$ and $\omega_-(w)$ are not plotted, correspond to the situation where the equilibrium value of the scaled coordinate $v_0(w, b)$ ceases to be real.)

For instance, in the case of $b = 3$, for $\mu = 8$, we observe resonances at the following five values of w: 0.02883, 0.1106, 0.2497, 0.9852, 0.9878. The critical value corresponds to the minimum of $\omega_+(w)$ for a given b in the interval $0 < w < w_1$ at the equilibrium point (the equilibrium scaled coordinate v being expressed via w by Eq. (4)). Calculating the derivative of ω_+ with respect to w and setting it equal to zero, we find the point of the minimum. The value of ω_+ at this point will be equal to the critical value of the scaled laser frequency μ_c. For example, for $b = 3$ at $w = 0.17642$ (the minimum of ω_+ in Figs. 3 and 4) this critical value is $\mu_c = 7.5944$. As the ratio of nuclear charges b increases, so does also the critical value μ_c of the scaled laser frequency.

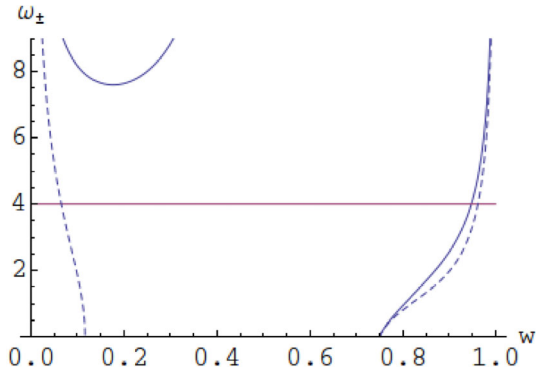

Fig. 3. Eigen-frequencies of the motion in the $z\rho$-space ω_+ (solid curves) and ω_- (dashed curves) versus w, i.e., versus the scaled z-coordinate of original circular Rydberg state. The scaled laser frequency μ is shown by the horizontal straight line. The plot is for $b = 3$ and $\mu = 4$. Three resonant points are seen.

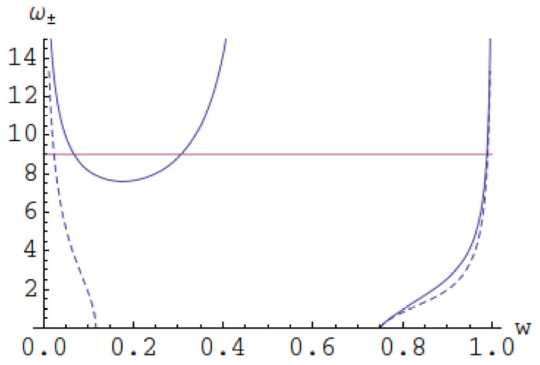

Fig. 4. Same as in Figure 3, but for $b = 3$ and $\mu = 9$. Five resonant points are seen.

These resonances correspond to a laser-induced unstable motion of the electron that result in the destruction of the helical states. This is illustrated in Figure 5 showing the calculated three-dimensional trajectory of the electron (for various directions of its initial velocity) for a resonance case where $b = 3$, $f = 1$, $\mu = 8$, and $w = 0.111$ ($w = 0.111$ is one of the three values of w, at which the laser frequency μ coincides with the eigen-frequency ω_+). A striking difference is seen compared to the stable helical motion depicted in Figure 2: the resonance destroyed the helical state – electrons are radially ejected.

3 Analytical solution for the case of a circularly-polarized laser field

Now we consider the case of a circular polarization of the laser field, polarization plane being perpendicular to the internuclear axis. The laser field varies as:

$$\mathbf{F} = F\,(\mathbf{e_x}\cos\omega t + \mathbf{e_y}\sin\omega t) \qquad (15)$$

where $\mathbf{e_x}$ and $\mathbf{e_y}$ are the unit vectors along the x- and y-axes, F is the amplitude and ω is the frequency.

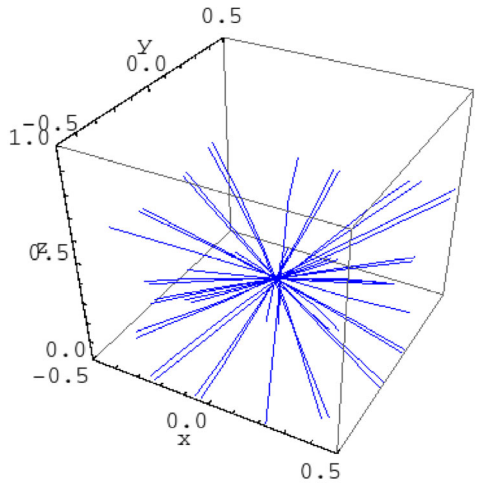

Fig. 5. The calculated trajectory of the electron (for various directions of its initial velocity) in the linearly-polarized laser field for a resonance case where $b = 3$, $f = 1$, $\mu = 8$, and $w = 0.111$. The z-axis is along the internuclear axis.

The Hamiltonian for the electron in this configuration will take the following form:

$$H = \frac{1}{2}\left(p_\rho^2 + p_z^2 + \frac{p_\varphi^2}{\rho^2}\right) - \frac{Z}{\sqrt{\rho^2+z^2}} - \frac{Z'}{\sqrt{\rho^2+(R-z)^2}} + F\rho\cos(\varphi-\varphi_0) \tag{16}$$

where we introduced $\varphi_0 = \omega t$. As in our paper [15], we consider φ-motion to be the rapid subsystem, i.e. $d\varphi/dt$ is much greater than the laser frequency ω and the frequencies of z- and ρ-motion. The canonical equations for the φ-motion obtained from equation (16) are:

$$\frac{d\varphi}{dt} = \frac{\partial H}{\partial p_\varphi} = \frac{p_\varphi}{\rho^2} \tag{17}$$

$$\frac{dp_\varphi}{dt} = -\frac{\partial H}{\partial \varphi} = F\rho\sin(\varphi-\varphi_0). \tag{18}$$

Combining (17) and (18), we get

$$\frac{d^2\varphi}{dt^2} = \frac{F}{\rho}\sin(\varphi-\varphi_0). \tag{19}$$

After a substitution $\varphi - \varphi_0 = \theta + \pi$, equation (19) becomes

$$\frac{d^2\theta}{dt^2} = -\frac{F}{\rho}\sin\theta \tag{20}$$

which is the equation of motion of a mathematical pendulum of length ρ in gravity F. Its two possible modes are libration and rotation; since θ is the rapid coordinate, we have the case of rotation. The solution for $\theta(t)$ is well-known and can be expressed in terms of Jacobi amplitude:

$$\theta(t) = 2\mathrm{am}\left(\frac{\Omega t}{2}, \frac{4F}{\rho\Omega^2}\right) \tag{21}$$

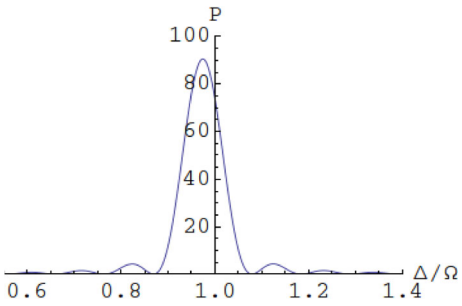

Fig. 6. The power spectrum of the electron radiation P (in arbitrary units) versus the dimensionless radiation frequency Δ/Ω for the case where $4F/(\rho\Omega) = 0.1$. Here Ω is the frequency of the electron radiation at the absence of the laser field. A certain width is assigned to all spectral components to display a continuous spectral line profile.

Here we denoted $d\theta/dt$ at $t = 0$ as Ω. For rapid rotations, the change in the angular speed on θ is insignificant compared to the initial speed and $d\theta/dt \approx \Omega$.

The expression for $\theta(t)$ enters the following Fourier-transform that determines the amplitude of the power spectrum of the electron radiation:

$$A_c\left(\Delta, \frac{4F}{\rho\Omega^2}\right) = \frac{1}{\pi}\int_0^\infty dt\cos\left(\Delta t - \theta\left(t, \frac{4F}{\rho\Omega^2}\right)\right). \tag{22}$$

Figure 6 shows as an example the power spectrum of the electron radiation spectrum (i.e., A_c^2) versus the dimensionless radiation frequency Δ/Ω for the case where $4F/(\rho\Omega) = 0.1$. It is seen that the most intense component in the spectrum is at the frequency Δ approximately equal to, but slightly less than Ω. It is also seen that the laser modulation of the primary frequency of the electron rotation results in a series of relatively small satellites of the primary spectral component.

The red shift of the primary spectral component can be calculated analytically as follows. Since φ-motion is rapid, we can average the Hamiltonian in equation (16) wth respect to time. Integrating equation (20) with the initial condition $d\theta/dt = \Omega$, we get

$$\Omega^2 - \left(\frac{d\theta}{dt}\right)^2 = \frac{4F}{\rho}\sin^2\frac{\theta}{2}. \tag{23}$$

By averaging this equation with respect to time, we obtain

$$\Omega^2 - \left\langle\left(\frac{d\theta}{dt}\right)^2\right\rangle = \frac{2F}{\rho}. \tag{24}$$

Thus, the φ-momentum term in the Hamiltonian (16) becomes

$$\left\langle\frac{p_\varphi^2}{\rho^2}\right\rangle = \rho^2\left\langle\left(\frac{d\theta}{dt}\right)^2\right\rangle = \rho^2\Omega^2\left(1 - \frac{2F}{\rho\Omega^2}\right) \tag{25}$$

The last term in the Hamiltonian from (16) vanishes after the time averaging so that the time-averaged Hamiltonian

depends only on ρ- and z-coordinates and their corresponding momenta. The result is the following quasi-stationary Hamiltonian with no explicit time dependence:

$$H=\frac{1}{2}\left(p_\rho^2+p_z^2\right)-\frac{Z}{\sqrt{\rho^2+z^2}}-\frac{Z'}{\sqrt{\rho^2+(R-z)^2}}+\frac{1}{2}\rho^2\Omega^2-\rho F. \tag{26}$$

Introducing the scaled quantities

$$w=\frac{z}{R},\ v=\frac{\rho}{R},\ f=\frac{FR^2}{Z},\ \sigma=\Omega\sqrt{\frac{R^3}{Z}} \tag{27}$$

and using the Hamiltonian equations, we obtain the following two differential equations of motion:

$$-\frac{d^2w}{d\tau^2}=\frac{w}{\left(w^2+v^2\right)^{3/2}}-\frac{b(1-w)}{\left((1-w)^2+v^2\right)^{3/2}} \tag{28}$$

$$-\frac{d^2v}{d\tau^2}=v\left(\frac{1}{\left(w^2+v^2\right)^{3/2}}+\frac{b}{\left((1-w)^2+v^2\right)^{3/2}}+\sigma^2\right)-f \tag{29}$$

(where the differentiation is by the scaled time $\tau = t(Z/R^3)^{1/2}$).

In this section we consider these Rydberg quasimolecules in circular (not helical) states, so that the plane of the electron orbit has a stationary position on the internuclear axis. Therefore, the right-hand side of equation (28) vanishes and the relationship between w and v becomes the same as given by equation (4). This makes the scaled radius of the orbit v a constant as well.

Since the angular momentum is $L = \Omega\rho^2$ for a stationary circular orbit, the averaging of the φ-momentum in equation (25) is equivalent to changing L for $L(1 - F\rho^3/L^2)$. Using scaled units and the relationship $L = \Omega\rho^2$, we find out that the case of the circularly-polarized laser field is equivalent to a field-free case, but with an effective frequency Ω given by the substitution:

$$\Omega \to \Omega\left(1-\varkappa(\gamma)f\right) \tag{30}$$

where

$$\varkappa(\gamma)=\frac{\gamma^6\left(\gamma^3-1\right)^{3/2}\left(\gamma^4-b^{2/3}\right)^{3/2}}{\left(\gamma^3+1\right)^{11/2}\left(b^{2/3}\gamma^2-1\right)^3}. \tag{31}$$

The quantity $\Omega\varkappa(\gamma)f$ is the red shift of the primary spectral component. This result is valid as long as the relative correction $\varkappa(\gamma)f$ to the unperturbed angular frequency Ω of the electron remains relatively small. Figures 7 and 8 illustrate the situation for the case where the ratio of the nuclear charges is $b = 2$. On the horizontal axis is the scaled coordinate w, i.e., the scaled coordinate along the internuclear axis of the Rydberg quasimolecule. The solid curve, having two branches, shows the unperturbed angular frequency Ω of the electron. The dashed curve shows the correction $\Omega\varkappa(\gamma)f$. It is seen that the correction remains relatively small for the entire left branch of Ω and

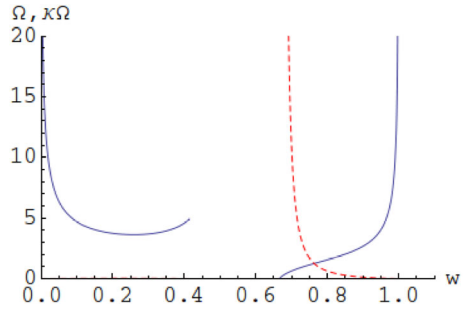

Fig. 7. Dependence of the unperturbed angular frequency Ω of the electron (solid curve, two branches) and of the correction $\Omega\varkappa(\gamma)f$ for $f = 1$ (dashed curve) on the scaled coordinate w along the internuclear axis of the Rydberg quasimolecule.

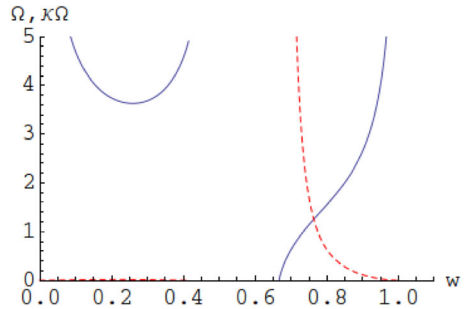

Fig. 8. The same as in Figure 7, but with better visible details in the region of the right branch of $\Omega(w)$.

for a significant part of the right branch of Ω. (Figs. 7 and 8 differ only by the range of the vertical scale, so that Fig. 7 allows to see more clearly the region where the solid and dashed curves intersect and the region of validity of the results for the right branch of Ω.) Physically, the left branch corresponds to the situation where the electron is primarily bound by the charge Z. The region of the right branch, where the correction is relatively small, physically corresponds to the situation where the electron is primarily bound by the charge Z'.

4 Conclusions

While studying diatomic Rydberg quasimolecules under a laser field that is linearly-polarized along the internuclear axis, we found an analytical solution for the stable helical motion of the electron valid for wide ranges of the laser field strength and frequency. Namely, the linearly-polarized laser field makes the motion in the $z\rho$-space to be forced oscillations at the frequency of the laser field. We also found resonances, corresponding to a laser-induced unstable motion of the electron, that result in the destruction of the helical states. For the situation where such Rydberg quasimolecules are under a circularly-polarized field, polarization plane being perpendicular to the internuclear axis, we found an analytical solution for circular Rydberg states valid for wide ranges of the laser field strength and frequency.

We showed that both under the linearly-polarized laser field and under the circularly-polarized laser field, in the electron radiation spectrum in the addition to the primary

spectral component at (or near) the unperturbed revolution frequency of the electron, there appear satellites. We found that for the case of the linearly-polarized laser field, the intensities of the satellites are proportional to the squares of the Bessel functions $J_q^2(s)$, $(q = 1, 2, 3, \ldots)$, where s is proportional to the laser field strength. As for the case of the circularly-polarized field, we demonstrated that there is a red shift of the primary spectral component – the shift linearly proportional to the laser field strength. We note that in quantum mechanics, spectral satellites can be best described using the formalism of quasienergy states, such as the states of the combined system "Rydberg quasimolecule + laser field" (see, e.g., [23]).

Under a laser field of a known strength, in the case of the linear polarization the observation of the satellites would be the confirmation of the helical electronic motion in the Rydberg quasimolecule, while in the case of the circular polarization the observation of the red shift of the primary spectral component would be the confirmation of the specific type of the phase modulation of the electronic motion described by equation (15). Conversely, if the laser field strength is unknown, both the relative intensities of the satellites and the red shift of the primary spectral component could be used for measuring the laser field strength.

References

1. G. Nogues, A. Lupascu, A. Emmert, M. Brune, J.-M. Raimond, S. Haroche, in *Atom Chips*, edited by J. Reichel, V. Vuletic (Wiley-VCH, Weinheim, Germany, 2011), Chap. 10, Sect. 10.3.3
2. N. Kryukov, E. Oks, Can. J. Phys. **90**, 647 (2012)
3. J.N. Tan, S.M. Brewer, N.D. Guise, Phys. Scr. **T144**, 014009 (2011)
4. N. Kryukov, E. Oks, Int. Rev. At. Mol. Phys. **3**, 17 (2012)
5. J.S. Dehesa, S. Lopez-Rosa, A. Martinez-Finkelshtein, R.J. Janez, Int. J. Quantum Chem. **110**, 1529 (2010)
6. T. Nandi, J. Phys. B **42**, 125201 (2009)
7. M.R. Flannery, E. Oks, Eur. Phys. J. D **47**, 27 (2008)
8. U.D. Jentschura, P.J. Mohr, J.N. Tan, B.J. Wundt, Phys. Rev. Lett. **100**, 160404 (2008)
9. A.V. Shytov, M.I. Katsnelson, L.S. Levitov, Phys. Rev. Lett. **99**, 246802 (2007)
10. M. Devoret, S. Girvin, R. Schoelkopf, Ann. Phys. **16**, 767 (2007)
11. M.R. Flannery, E. Oks, Phys. Rev. A **73**, 013405 (2006)
12. E. Oks, Eur. Phys. J. D **28**, 171 (2004)
13. L. Holmlid, J. Phys.: Condens. Matter **14**, 13469 (2002)
14. E. Oks, Phys. Rev. Lett. **85**, 2084 (2000)
15. E. Oks, J. Phys. B **33**, 3319 (2000)
16. S.K. Dutta, D. Feldbaum, A. Walz-Flannigan, J.R. Guest, G. Raithel, Phys. Rev. Lett. **86**, 3993 (2001)
17. H. Carlsen, O. Goscinski, Phys. Rev. A **59**, 1063 (1999)
18. J.E. Rice, E.S. Marmar, J.L. Terry, E. Källne, J. Källne, Phys. Rev. Lett. **56**, 50 (1986)
19. G.R. Fowles, G.L. Cassiday, in *Analytical Mechanics* (Thomson Brooks/Cole, Belmont, 2005), Sect. 3.6
20. S.T. Thornton, J.B. Marion, in *Classical Dynamics of Particles and Systems* (Thomson Brooks/Cole, Belmont, 2004), Sect. 3.6
21. I.I. Sobelman, *An Introduction to the Theory of Atomic Spectra* (Pergamon, Oxford, 1972)
22. D.I. Blochinzew, Phys. Z. Sow. Union **4**, 501 (1933)
23. E. Oks, in *Plasma Spectroscopy. The Influence of Microwave and Laser Fields* (Springer, New York, 1995), Sect. 3.1